Future stem cell analysis: Progress and challenges towards state-of-the art approaches in automated cells analysis.

Nurul Syahira Mohamad Zamani [1] , **Wan Mimi Diyana Wan Zaki** [Corresp., 1] , **Zariyantey Abd Hamid** [2] , **Aqilah Baseri Huddin** [1]

[1] Faculty of Engineering and Built Environment, Universiti Kebangsaan Malaysia, Department of Electrical, Electronic and Systems Engineering, UKM Bangi, Selangor, Malaysia

[2] Faculty of Health Sciences, Universiti Kebangsaan Malaysia, Biomedical Science Programme and Centre for Diagnostic, Therapeutic and Investigative Science, Kuala Lumpur, W. P. Kuala Lumpur, Malaysia

Corresponding Author: Wan Mimi Diyana Wan Zaki
Email address: wmdiyana@ukm.edu.my

Background and aims. A microscopic image has been used in cell analysis for cell type identification and classification, cell counting and cell size measurement. Most previous research works are tedious, including detailed understanding and time-consuming. The scientists and researchers are seeking modern and automatic cell analysis approaches in line with the current in-demand technology.

Objectives. This paper provides a brief overview of a general cell and specific stem cell analysis approaches from the history of cell discovery up to the state-of-the-art approaches.

Methodology. A content description of the literature study has been surveyed from specific manuscript databases using three review methods: manuscript identification, screening, and inclusion. This review methodology is based on Prism guidelines in searching for originality and novelty in studies concerning cell analysis.

Results. By analysing generic cell and specific stem cell analysis approaches, current technology offers tremendous potential in assisting medical experts in performing cell analysis using a method that is less laborious, cost-effective, and reduces error rates.

Conclusion. This review uncovers potential research gaps concerning generic cell and specific stem cell analysis. Thus, it could be a reference for developing automated cells analysis approaches using current technology such as artificial intelligence and deep learning.

Future Stem Cell Analysis: Progress and Challenges Towards State-of-the art Approaches in Automated Cells Analysis

Nurul Syahira Mohamad Zamani[1], W Mimi Diyana W Zaki[1], Zariyantey Abdul Hamid[2], Aqilah Baseri Huddin[1]

[1] Department of Electrical, Electronic and Systems Engineering, Faculty of Engineering and Built Environment, Universiti Kebangsaan Malaysia, Selangor, Malaysia
[2] Center for Diagnostic, Therapeutic and Investigative Studies, Faculty of Health Sciences, Universiti Kebangsaan Malaysia, Kuala Lumpur, Malaysia

Corresponding Author:
W Mimi Diyana W Zaki[1]
Faculty of Engineering & Built Environment, Universiti Kebangsaan Malaysia, 43600 UKM, Bangi Selangor, Malaysia
Email address: wmdiyana@ukm.edu.my

Abstract

Background and aims. A microscopic image has been used in cell analysis for cell type identification and classification, cell counting and cell size measurement. Most previous research works are tedious, including detailed understanding and time-consuming. The scientists and researchers are seeking modern and automatic cell analysis approaches in line with the current in-demand technology.

Objectives. This paper provides a brief overview of a general cell and specific stem cell analysis approaches from the history of cell discovery up to the state-of-the-art approaches.

Methodology. A content description of the literature study has been surveyed from specific manuscript databases using three review methods: manuscript identification, screening, and inclusion. This review methodology is based on Prism guidelines in searching for originality and novelty in studies concerning cell analysis.

Results. By analysing generic cell and specific stem cell analysis approaches, current technology offers tremendous potential in assisting medical expert in performing cell analysis using a method that is less laborious, cost-effective, and reduces error rates.

Conclusion. This review uncovers potential research gaps concerning generic cell and specific stem cell analysis. Thus, it could be a reference for developing automated cells analysis approaches using current technology such as artificial intelligence and deep learning.

36 Introduction

37 The etymology term 'cell' was coined in the scientific study using a microscope as early as 1665.
38 Over two centuries have passed, and the term stem cell arose in 1868 to describe an organism's
39 evolvement of a fertilised egg. Numerous laboratories study cells incorporating cells analysis has
40 been conducted over the 19th and 20th centuries until the World War II incident. This incident
41 contributed to the first stem cell transplantation of bone marrow and hematopoietic cell
42 discovery (Mathe', 1959) and repeated experiment works (Gregory et al., 1968; Jacobson et al.,
43 1949; Jacobson et al., 1951). Stem cells are mainly categorised into embryonic stem cells
44 (ESCs), adult stem cells, and induced pluripotent stem cells (iPSCs), which can be further
45 classified according to differentiation potency known as totipotent, pluripotent, multipotent,
46 oligopotent, and unipotent. Stem cells generate tissues through their differentiation potency,
47 forming mature and functioning cells while retaining stem cells' pool size via self-renewing
48 ability. Adult stem cells and iPSCs play a greater role in medicine for the regeneration and repair
49 of damaged tissue than ESCs, which are hampered by ethical issues (Seita & Weissman, 2010).
50   To date, hematopoietic stem cells (HSCs) are among the best-characterised adult stem
51 cells with known multipotency properties (Lin, Otsu & Nakauchi, 2013). Having a remarkable
52 regenerative potential, HSCs have been widely and successfully used for therapeutic purposes
53 via bone marrow and HSCs transplants (Hamid et al., 2020), a standardised stem cell therapy for
54 haematological diseases such as aplastic anaemia, leukaemia, and immunodeficient disorders.
55 Apart from HSCs, iPSCs utilisation also confers excellent therapeutic potential, particularly in
56 regenerative medicine (Yuasa & Fukuda, 2008). Cell-based assays using iPSCs have been used
57 for new drug development and toxicity screening. Since iPSCs possess similar stem cells potency
58 as acquired by embryonic stem cells, they are becoming a favourable source of stem cells being
59 used in clinical testing for drug screening, disease modelling, and cell-based therapy (Fakunle &
60 Loring, 2012; Tanaka et al., 2014; Avior, Sagi & Benvenisty, 2016; Kusumoto, Yuasa &
61 Fukuda, 2022).
62   Before application in research and stem cell-based therapy for regenerative medicine,
63 stem cells' potency and function must be identified and confirmed, often requiring a trained
64 scientist or operator to conduct the analysis. The requirement for microscopic observation and
65 manual analysis of stem cell characteristics is fundamental in specific analytical procedures.
66 However, these procedures are mainly performed using conventional methods (Ramakrishna et
67 al., 2020). For example, functional characterisation analysis of HSCs and iPSCs requires
68 microscopic identification and classification of colony subtype via colony-forming assay. A
69 trained operator must perform this conventional approach; laborious, time-consuming, and prone
70 to errors in data reporting. Hence, this review study is intended for clinicians, scientists, and
71 researchers recently enlightened about automated systems to analyse generic cell and stem cells,
72 particularly in HSCs, iPSCs, and other cell types. This automated system could foster and
73 empower stem cell research and its application for therapy.

74   Therefore, an introduction to this review study of the generic cell and stem cell analysis is
75 briefly explained in this paper. In this review, we present a literature study based on
76 methodology concerning article selection as described in Section 2. In Section 3, we provide an
77 overview of the beginning of cell and stem cells, followed by a brief explanation regarding cell
78 analysis evolution back in the 16th century towards the state-of-the-art analysis approaches in the
79 21st century, including bacterial colonies in microscopic images in Section 4. Then, fully
80 developed cell colonies and stem cell analysis system will be thoroughly explained in Section 5.
81 Finally, a summary of the overview of stem cells and the execution of automated analysis using
82 deep learning will be the concluding remarks of this review, as disclosed in Section 6.

Survey methodology

84 A literature survey on a particular subject was performed to filter and review the evolution of
85 various approaches for general cell analysis. In this study, we aim to understand and systemise
86 the reviewed publications from the top list of academic search engines, which are Google
87 Scholar and selected publisher databases with citation index traced by SCIMAGO journal
88 ranking. For example, Elsevier, IEEE Xplore, Web of Science, and several primal publishers
89 such as JSTOR for certain manuscripts, including Dutch manuscripts, for originality and novelty
90 concerning cell analysis approaches. For the primal publisher, some ancient manuscripts require
91 extra effort to understand the author's lengthy and indirect explanations. Therefore, time period
92 restrictions were applied for historical evolution studies from the 16th century to the current
93 evolution study in the 21st century. By referring to guidelines to systemise review, such as the
94 origin of stem cells (Ramalho-Santos & Willenbring, 2007), microscope inventions (Hajdu,
95 2002) and cell analysis evolution (Mitra-Kaushik et al., 2021), including technical journals for
96 advanced cell analysis. This part consists of various types of cell analysis, such as traditional
97 (manual and clinical practice), conventional (image processing and machine learning), and state-
98 of-the-art (deep learning).
99   The publications were selected according to the inclusion and exclusion criteria of the
100 most appropriate manuscripts from the mentioned databases. Three inclusion criterions were
101 involved in this review, starting with the identification phase, followed by screening and
102 inclusion phase. A total of 183 articles were selected and identified with appropriate title
103 manuscripts contributed to cell analysis. Then, the screening phase is based on the contents of
104 the abstract and keywords such as "microscope", "stem cell", "single-cell analysis", "cell
105 identification", "cell counting", "image processing", "machine learning" and "deep learning".
106 Roughly 65 of 183 articles were sorted out, and about 118 were sorted in for downstream data
107 extraction. Finally, 101 articles were extracted for references throughout this review study. The
108 review articles in the cell analysis evolutions section and the research articles without complete
109 results were excluded for exclusion. To be noted, Mendeley has been used as a citation Software
110 manager. Figure 1 illustrates the article's inclusion and exclusion process for this review based
111 on Prisma guidelines (Abdolrasol et al., 2021; Miah et al., 2022).

112 An overview of cells and stem cells

113 In the late 1950s and early 1960s, a multidisciplinary work between two scientists, a cellular
114 biologist and a biophysicist, Ernest McCulloch and James Till, conducted scientific research on
115 the susceptibility of mice bone marrow tissue to radiation exposure (McCulloch & Till, 1960).
116 From nuclear accidents, scientists acknowledge and theorise that there is something in the blood
117 that can treat cancer or radiated cells from healthy cells. Both scientists injected healthy mice
118 bone marrow cell transplantation into irradiated mice. Afterwards, they noticed small lumps
119 representing a colony appearing on blood filter cells called the spleen of mice (Till & Mcculloch,
120 1961). The appearance of small lumps is known as hematopoietic stem cells (HSCs). This
121 experiment has been conducted repeatedly to understand the sensitivity of healthy cells in mice
122 bone marrow to radiation (McCulloch & Till, 1962) and cytological evidence between both cells
123 (Wu et al., 1968). Through repeated experiments, scientists discovered stem cells from spleen
124 colonies in bone marrow, which shows that a single cell can produce colonies by direct cytology
125 (Till & Mcculloch, 1961; McCulloch & Till, 1962; Becker, Mcculloch & Till, 1963;
126 Siminovitch, Mcculloch & Till, 1963). A stem cell has self-renewal ability and differentiates into
127 a new cell categorised into multipotent stem cells. The HSCs are responsible for the
128 differentiation of the blood cells such as erythrocyte (red blood cell), leukocyte (white blood
129 cell), and platelet cell lineages through the hematopoiesis process (Wu et al., 1968; Chow et al.,
130 2021). The hematopoiesis process has been practically demonstrated in nuclear survivors and
131 irradiated mice bone marrow transplants. Therefore, it is very crucial to maintain hematopoiesis
132 with HSC differentiation (Dewi et al., 2020).
133   Stem cells proliferate through self-renewal division and develop into contrasting or
134 specialised cell types. Self-renewal is the stem cell division process to generate more stem cells,
135 and multi-lineage differentiated progenitors while preserving the undifferentiated state of new
136 stem cells (Worton, Mcculloch & Till, 1969; Weissman, 2000; Kolios & Moodley, 2013; Lin,
137 Otsu & Nakauchi, 2013). Undifferentiated cells define the state of immature cells that have not
138 yet been assigned to specific cells function. The evolutions of stem cells are based on single cell
139 (clonal), where the changing process refers to differentiation and potency to form specific and
140 different cell types and tissue (Coulombel, 2004; Loya, 2014; Łos, Skubis & Ghavami, 2018).
141 The established form of stem cells is embryonic stem cells (ESCs) and adult stem cells (ASCs).
142 Furthermore, stem cells can be further classified based on their differentiation potency and
143 origin. Potency refers to stem cells' ability to differentiate into different types of cells (have a
144 specialised function). Regarding potency, stem cells are divided into five main categories:
145 totipotent, pluripotent, multipotent, oligopotent, and unipotent (Maleki et al., 2014). The highest
146 hierarchy in differentiation potential of a stem cell is known as totipotency which enables a
147 single stem cell to generate embryo and extra-embryonic tissues (Kolios & Moodley, 2013;
148 Zakrzewski et al., 2019). An example of a totipotent stem cell is a fertilised egg (zygote).
149   The second stage of stem cell potency is called pluripotent stem cells (PSCs), whereas a
150 form of blastocyst's inner cells masses from four days of zygote formation. Pluripotent stem cells

151   can divide and differentiate into three germ layers: ectoderm, endoderm, and mesoderm
152   (Weissman, 2000; Lin, Otsu & Nakauchi, 2013), all of which are derived from ESCs.
153   Reprogrammed somatic cells, induced pluripotent stem cells (iPSCs), are the first artificially
154   generated stem cells to mimic the function of ESCs (Takahashi & Yamanaka, 2006; Zakrzewski
155   et al., 2019). Since then, iPSCs have been regarded as the popular pluripotent stem cells used in
156   stem cell research and therapy. The multipotent stem cell has restricted differentiation potency
157   compared to ESCs and iPSCs. Mesenchymal stem cells (MSCs) and HSCs are an example of
158   multipotent stem cells due to their ability to differentiate into multi-lineage and multiple types of
159   cells. HSCs can further differentiate to form oligopotent stem cells/progenitors with limited
160   differentiation ability to form cells for specific lineage, such as myeloid and lymphoid (Ebihara
161   et al., 1997; Coulombel, 2004). Finally, fully specialised cells that can reproduce to generate
162   more tissue-specific cells are defined as unipotent stem cells such as skin, cornea, muscle,
163   pancreas, etcetera (Tatullo et al., 2019).

164 Evolution of cell analysis approaches

165   This section describes the cell analysis starting with the history, which prescribes the origin of
166   the cell discovery through the invention of microscope observation in the 16th century (Ball,
167   1966; Hajdu, 2002; Ponti & Muscatello, 2015. The cell analysis approaches evolved using a
168   photoelectronic method by counting cells through flowing fluid, gas and light with a generated
169   electronic pulse (Moldavan, 1934; Coons, Creech & Jones, 1941; Gucker Jr et al., 1947; Guyton,
170   1946; Gucker & O'Konski, 1949; Crosland-Taylor, 1953; Coulter, 1953; Graham, 2003), and the
171   counted cells can be sorted out according to their cell type using the cell sorter method (Mie,
172   1908; Twersky, 1964; Fulwyler, 1968; Wyatt, 1969; Bonner et al., 1972; Wyatt et al., 1988). The
173   approaches have progressed as technology emerged in the late 20th and early 21st centuries.
174   Digital image processing (DIP) has paved the way for microscopic image analysis using
175   processing unit capability with the help of camera technology. Nevertheless, the development of
176   technology evolved to meet the high demand requirement, which included the automated
177   approaches of cell analysis using deep learning. Figure 2 illustrates the evolution of the history to
178   the current cell analysis approaches.

179 The history of cell analysis (from 16th century)

180   *Microscope inventions:* In the early 1600s, Galileo made a microscope to observe minuscule
181   things representing microorganisms (Haden, 1939, 1942). Later in 1665, Robert Hooke invented
182   a simple single lens of the microscope, as illustrated in Fig. 3. One of Hook's discoveries was
183   when he examined a thin slice of the cork, a dead tissue found in the bark tree that looked like a
184   honeycomb. Hooke expressed his vision on the first microscopical stoma, where the term 'cell'
185   was coined to describe the building blocks of living things, the etymology of the word used in
186   biology. After a decade had passed, Antoni van Leeuwenhoek discovered the first detailed cell

187   description specified the living cells of bacteria and protist parasites as well as the red blood cell
188   as he continued blood capillaries observation by Marcello Malpighi back in the early 1660s
189   (Harris, 1911; Packard, 1928; Saraf & Cockett, 1984; Leeuwenhoek, 1677; Lane, 2015).
190   *Photoelectronic techniques:* Moldavan has proposed a photo-electric system for microscopical
191   cell counters (Moldavan, 1934). Early bacteriologists used this method to estimate the number of
192   bacteriophages, enzymes, and viruses. This approach aims to have the photo-electric tool
193   automatically record the presence of each microscopical cell flowing through the capillary tube
194   to amplify the generated micro-current. In the mid of 1950s, a principle of automated cell
195   counting called the Coulter Principle was proposed inspired by Moldavan's microscopic
196   observation of photo-electric cell counting passing through a capillary (Coulter, 1953). A few
197   years later, Wallace introduced an automatic system of blood cell counters that made cell
198   distribution size faster (Coulter, 1956), as shown in Fig. 4.
199   *Cell sorter techniques:* Various modalities have carried out the evolution of cell analysis
200   in the past. The cell sorter technique is generally used to analyse the physical characteristics of
201   cells or particles using flow cytometry and flow sorting method (Fulwyler, 1968; Cram & Arndt-
202   Jovin, 2005). Fluorescence has been widely used in biology for cell stains marker. The
203   quantitative measurement of cell fluorescent emissions light called the cell microfluorometry
204   method (Van Dilla et al., 1969). In 1972, Bonner et al. introduced a rapid instrument for
205   biological cell sorting analysis called a flow cytometry technique. The cells with different
206   fluorescent compounds are injected into a narrow tube of a flowing stream and lighted up with a
207   laser beam, as illustrated in Fig. 5. The fluorescent compounds used in this instrument include
208   fluorescence, quinacrine mustard, and acridine orange (Bonner et al., 1972). Table 1 lists the
209   evolution of cell analysis from a historical point of view from the microscope invention prior to
210   photoelectronic and cell sorter techniques. In summary, this historical review describes the
211   invention and proposed approaches from the origin of single-cell identification in the 16th
212   century until pre-modern cell analysis techniques in the 20th century. By analysing the
213   approaches, the research potential and gap could be determined for future research suggestion
214   improvement.

Cell analysis using DIP and machine learning approaches (from
216   19th century)

217   In a literature study, the naked eye discovered the image of single-cell identification through
218   microscope observation. In other words, the discovery was carried out with eyes vision.
219   Although the inability to analyse the invisible data (visualisation) could be saved in brain
220   memory with the help of the retina through the optic nerve, the illustration can be retrieved
221   through a sketch. This analogy from a pair of biological cameras has been a commence which
222   brings to the beginning of the physical cameras that can capture the image instantly and store it
223   in physical memory.

224   DIP focuses on improving image representation for machine interpretation with image
225   analysis purposes that led to the start of computer vision until today. Computer vision consists of
226   a digital image processing approach that has performed several machine learning techniques.
227   Machine learning is a subset of artificial intelligence (AI) that enables the programmed system
228   with an algorithm to analyse data from a learning experience (Zamani et al., 2020). Previous
229   studies have paved the way in cell analysis study including detection, counting, cell size
230   measurement, and cell sorting. However, all the experiments have been performed clinically and
231   conducted with expertise. Nonetheless, a scientist has developed physical instruments and
232   devices for practical use. Regardless of this benefit, most of the equipment is expensive and
233   inappropriate for researchers for trial and error. Various cell analysis approaches have been
234   proposed for image detection and classification using image processing and machine learning in
235   the late 20th and early 21st centuries. For example, single smooth muscle cells have been acquired
236   using a developed digital imaging microscope by utilising fluorescence probes (Fay, Carrington
237   & Fogarty, 1989). The acquired three-dimension dataset was analysed with the optic processing
238   reverses distortion to identify the characteristic of an image region. In 2002, an analysis of white
239   blood of various lineage and maturity was performed (Hengen, Spoor & Pandit, 2002). The
240   morphological feature was applied in feature extraction, where the nucleus cell's structure was
241   analysed using watershed transform and Gabor filter; meanwhile, the cell shape was analysed
242   using rotational invariant contour. Based on these features, the Gaussian-Bayesian classifier was
243   used for classification.
244   Haematoxylin and eosin-stained (H&E) image gas was automatically identified using two
245   neural network layers with a 10-fold cross-validation technique (Bhagavatula et al., 2010). H&E
246   staining helps in cell identification and provides cell information, such as the shape of cell tissue.
247   The result shows that accuracy classification gives an average of about 74.9% to 93.2% using
248   pixel-based classification. In 2012, Lowry et al. performed a multi-stage Bayesian level
249   algorithm to segment the iPSC colony (Lowry et al., 2012). Some of the colonies were
250   misclassified, but apparently, the tested iPSCs have been successfully segmented. Guan et al.
251   classify human embryonic stem cells (hESCs) using statistical Gabor descriptors and show they
252   classify more accurately than histogram-based features (Guan et al., 2014). A stem cell marker
253   has been proposed to detect cancer stem cells in the microscopic image using a CD13 staining
254   marker (Oğuz et al., 2015). Oğuz et al. applied a support vector machine (SVM) to classify
255   cancer stem cell images and successfully developed CD13 positive cancer stem cells marker on
256   the microscopic image. In 2018, a mesenchymal stem cell (MSCs) classification was performed
257   based on feature extraction using Wavelet and classified using SVM, resulting in greater
258   accuracy than information gain and genetic algorithm techniques (Sreedevi & Pachaiammal,
259   2018).
260   Hyperspectral imaging (HSI) microscopy is a 2D image technique used in biomedical
261   imaging for cell analysis. Ogi et al. (Ogi et al., 2019) have developed a highspeed HSI method to
262   classify neural stem cells with 94% precision using pixel-wise ML. In 2020, a cell classification
263   platform for human PSCs (hPSCs) was proposed for cell-based therapy from the cell's glycome

264 using a supervised ML approach (Shibata et al., 2020). Shibata et al. employed linear
265 classification and neural network to classify five classes of annotated lectin microarray data from
266 hPSCs: mesenchymal stromal cells, endometrial cells, endometrial and ovarian cancer cells,
267 cervical cancer cells and pluripotent stem cells. Both supervised ML approaches have achieved
268 89% and 97% accuracies, respectively, for the hPSCs classification system. Recently, the ML
269 approach has also been implemented to predict allogeneic stem cell donors from the granulocyte
270 colony-stimulating factor (G-CSF) of HSC (Xiang et al., 2022). The established prediction
271 methods were performed by cross-validation (10-fold) with appropriate hyper-parameter using a
272 grid search technique. The best ML prediction models are random forest and AdaBoost with the
273 area under the curve (AUC), 89% and 88% scores, respectively, compared to a decision tree,
274 linear regression, SVM, feedforward neural network and gradient boosting.
275   Image processing and ML have been widely implemented in microscopic images with
276 benefits based on their reliability and robust technique. However, the accuracies of image
277 analysis depend on the techniques and experiences of the researchers. Furthermore, image
278 processing and machine learning approaches are laborious to find the most significant image
279 features with the appropriate algorithm, which is very time-consuming.

280 Automated cell analysis using deep learning (21st century)

281 Previous and current studies have proposed and suggested the appropriate experimental work for
282 image analysation through a deep neural network (DNN). A test analysis of the stem cells in the
283 form of a microscopic image where the type of cells is rationally needs to be validated by the
284 cells specialist (cytobiologist).
285   An automated assessment of stem cells approach gives rise to DNN in
286 recognition/classification of HSCs and iPSCs colonies, although there is minimal comprehensive
287 study related to these stem cell colonies. In 2017, Kavitha et al. developed a new vector-based
288 convolutional neural network (V-CNN) to classify feature vectors of healthy and unhealthy
289 colonies by differentiating features of the colony (Kavitha et al., 2017). Before V-CNN
290 classification, the colony undergoes image segmentation and feature measurement to compute
291 morphological and texture features. This segmentation achieved a robust segmentation.
292 However, it is challenging to compute the segmented colony region for the ensuing stem cell
293 characteristics measurement (Paduano et al., 2013). The proposed V-CNN classification
294 performance was then compared to SVM classifier by five-fold cross-validation. The
295 performance of V-CNN achieved high accuracy above 90%, while the SVM classifier had only
296 77% accuracy. Therefore, V-CNN has outperformed the conventional classifier (SVM), which
297 has a high potential for a reliable framework for automated recognition of iPSCs colonies.
298   A primary hematopoietic progenitor identification was proposed in the same year by
299 differentiating lineage choice prediction using DNN on image patches from brightfield
300 microscopy and cellular movement (Buggenthin et al., 2017). The hematopoietic progenitor stem
301 cells are differentiated into granulocytic/monocytic lineage (GM) and megakaryocytic/erythroid
302 lineage (MegE). The idea of the CNN combination is to extract the image features automatically

303   with long short-term memory (LSTM) of recurrent neural network (RNN) architecture for cell

304   dynamics models. A proposed CNN was adopted from the LeNet structure with three

305   convolutional layers, a nonlinear activation function: ReLU (alternately after the convolutional

306   layer), a max-pooling layer, and two fully connected layers. The limitation of DNN deployments,

307   such as overfitting during the network training, Buggenthin and the team have overcome the

308   problem by using dropout layers after a fully connected layer where the weight of the unwanted

309   features is discarded. Then, the annotated cells (visible cell marker) and latent cells (non-visible

310   cell marker) are fed into a softmax classifier for classification purposes. For an RNN, the output

311   of the extracted features is transferred to an LSTM with 20 hidden nodes. The CNN-RNN

312   proposed method predicts the three-lineage choice of hematopoietic progenitor with fast and

313   robust for new data as it is applied with a low-level feature calculation. On average, the area

314   under the curve (AUC) performance with 87.3% for annotated cells and 79.3% for latent cells.

315   The CNN implementation has shown a remarkable performance in the morphological

316   identification of iPSCs and haematopoietic cells. Human iPSCs represent an experimental model

317   for cell development. A deep learning CNN architecture was implemented to automatically

318   classify and recognise iPSC regions in microscopy images (Chang et al., 2017). The microscopy

319   image of iPSCs was divided into six classes based on cell patterns. The six regions are with no

320   cells, separate cells, unclustered cells, clustered cells, tightly clustered cells, and regions with

321   iPSCs. Five convolutional layers and two fully connected layers are used for CNN architecture.

322   Overall, the classification of six classes archived Top-1 9.2% and Top-2 0.84% of error rates

323   with average time execution of approximately 0.076 seconds.

324   Kusumoto et al. (2018) have proposed identifying endothelial cells derived from iPSCs

325   without immunostaining or lineage trace requirements. To establish an automatic prediction, they

326   implement two DNN architectures: LeNet contains two layers of the convolutional network, max

327   pooling and fully connected, respectively, and AlexNet with five convolutional layers and three

328   max pooling and fully connected layers. A total of 800 images were used, 600 for training and

329   200 for validation. The network parameter was optimised to increase prediction accuracy and

330   validated by K-fold cross-validation. The identification achieved 70% for both accuracy and F1

331   score (LeNet) and AlexNet score 90% accuracy and 75% F1 score. Based on the network

332   performance, the network depth and pixel size's image play an important role in correlating the

333   prediction accuracy. In 2020, a microscopic image of erythrocytes was acquired using mobile

334   microscopy and automatically segmented to identify malaria using a deep residual network

335   (ResNet) (Pattanaik et al., 2020). ResNet is one of the DNNs modified with the adoption of batch

336   normalisation implemented after the convolutional layers works. The modified network called

337   multi-magnification ResNet (MM-ResNet) was fed with multi-magnification of microscopic

338   images of 200x, 400x and 1000x magnification. The proposed system has achieved slightly low

339   accuracy (0.10%) compared to GoogleNet. Despite that, the proposed system beats the test error

340   rate of GoogleNet with 19.93% compared to 25.86%.

341   Researchers have recently proposed a classification/identification of bacterial colonies in

342   another type of microorganism with the same culture in microscopic images as HSCs and iPSCs;

343   researchers have recently proposed a classification/identification of bacterial colonies. Early
344   detection and classification of bacterial colonies have been proposed using pseudo-three
345   dimensional (3D) of DenseNet (Wang et al., 2020). The images of live bacteria colonies are
346   captured by a monochromatic complementary metal-oxide-semiconductor (CMOS) image sensor
347   after being incubated for 24 hours in four time-consecutive frames in each time-lapse imaging
348   for detection purposes. A total of 6969 E. coli, 2613 K. aerogenes, and 6727 K. pneumoniae are
349   the estimated images used for the training model, and about 965 colonies were tested of the three
350   classes. All the images were augmented with rotation by 90 degrees and flipping randomly. The
351   authors modified the DenseNet architecture by replacing two-dimensional (2D) convolutional
352   layers with three-dimensional convolutional layers. The modified network was then randomly
353   initialised with a hyper-parameter learning rate of 0.0001, batch size of 64, and optimised by an
354   adaptive moment estimation optimiser (Adam). While training the data, the learning rate was
355   decayed by half for every 20 epochs to stabilise the network accuracy. For classification
356   purposes, the images used only contained true classes of about 9400 growing colonies with the
357   same hyper-parameter setting except for the learning rate decaying during the network training
358   by 0.9 for every ten epochs. The training process for classification took 10 hours more than the
359   detection task, resulting in 80% (classification) and 95% (detection) using the same environment
360   of dual graphic processing units (GPUs) (GTX1080Ti) Nvidia. Despite the small number of
361   training data used in classification resulting in low accuracy, it took more time to process, which
362   proved that the network probably encountered an underfitting problem.
363   Two years later, another experimental work has been proposed using the same network
364   architecture and bacterial colonies classes as (Wang et al., 2020) DenseNet by replacing the 2D
365   convolutional layer with pseudo-3D convolutional layers except for the hyper-parameter settings.
366   The authors (Li et al., 2022) have demonstrated the first use of a real-time detection system with
367   a thin-film-transistor (TFT)-based image sensor by automatically counting and identifying CFU
368   species using a deep learning approach. Unlike Wang et al., the TFT-based image sensor is field-
369   portable as there is no requirement for image scanning on an agar plate and time effective as the
370   image was taken within 5 minutes. A total of 889 colonies of positive class and 159 colonies of
371   the negative class were augmented by rotation and flipping as well as Wang et al. performed
372   training, and another 442 colonies (positive class) and 135 colonies (negative class) were
373   assigned for testing. This experimental work has performed by 5-fold cross-validation with the
374   hyper-parameter setting of 0.0001 learning rate and batch size of 8, and the network was
375   scheduled to decrease the learning rate by 0.8 for every ten epochs and optimised by Adam
376   optimiser. As for the classification task, the authors assign 442 colonies which are less than the
377   detection task with the same network architecture but have a contrast for the hyper-parameter
378   setting. Regardless of the less training data used and time-effective, this experimental work has
379   achieved 92.6% sensitivity and 100% specificity (detection), and 100% classification accuracy,
380   which has been improved from previous work in 2020. This achievement shows that despite the
381   total training data and balancing data used, the combination of hyper-parameter selection is vital
382   for converging the network and avoiding overfitting and underfitting problems in deep learning.

383   Manual work to count the CFUs was laborious, time-consuming, and prone to error. A
384   bacterial colonies detection has been proposed and aimed to automate the CFU cell counting
385   using U-Net architecture for vaccine development (Beznik et al., 2022). The CFUs were grown
386   from the number of viable and proportion of virulent bacterial colonies that were cultured on a
387   blood agar plate. A plate of CFU consists of four classes, namely bgv+ colony (virulent), bgv-
388   colony (avirulent), background, and border from 108 images. From the point of view, the
389   researchers have highlighted the challenges in deep learning apart from millions of parameters
390   and large-scale data requirements; they also encountered the imbalance of data as the petri dish
391   image mostly represented by background class and solved it by altering the loss, and the image
392   noise such as reflections from light-emitting diodes (LEDs). This work implements two networks
393   of regular U-Net (Ronneberger, Fischer & Brox, 2015) with a batch normalisation layer and pre-
394   trained U-Net from ResNet, Inception-ResNet, and DenseNet (Russakovsky et al., 2015) in
395   search for the best hyperparameter combination. These models have been trained using three
396   learning rates (0.001, 0.0001, and 0.00001), batch size of 8, epochs 10, and Adam optimiser.
397   ResNet-152 has outperformed other models for cell counting with learning rate of 0.0001 with
398   precision and recall achievement, bgv+ (90.6%, 92.7%) and bgv- (91.9%, 90.5%), respectively.
399   However, the proposed framework has scored less than 74.5% for true positive class detection,
400   which is quite low for state-of-the-art performance. This result is probably due to the small-scale
401   training data used with the deep layer network such as ResNet and DenseNet, and imbalanced
402   data that leads to the underfitting problem.
403   Data imbalance is a well-known scenario in medical imaging when training using a deep
404   neural network (Johnson & Khoshgoftaar, 2019; Cano et al., 2021). Zhang et al., 2022 used a
405   balanced total data sample for training and testing to identify three bacteria classes to overcome
406   this problem. A total of 3059 images of Salmonella Enteritidis, 3110 images of Salmonella
407   Paratyphoid, and 3092 images of Salmonella Typhimurium were used in this work. These are the
408   number of surface-enhanced Raman spectroscopies (SERS) spectral samples of bacteria in the
409   water bath. All the SERS samples were fed to seven different architectures. Regardless, the
410   authors did not mention the hyper-parameter used in this experimental work training process for
411   evaluation purposes. Despite that, the stacking-CNN has been well-converged at epochs 15
412   without experiencing an overfitting problem. This model has outperformed other architectures
413   with the accuracy of 98.41% (Salmonella Enteritidis), 97.89% (Salmonella Paratyphoid), and
414   98.31% (Salmonella Typhimurium). This work shows that balancing data could help achieve
415   excellent performance despite the combination of hyper-parameter during the training process.
416   In summary, Fig. 6 illustrates the Venn diagram briefly explaining each field. It shows the
417   relationship between computer vision representing image processing approaches with artificial
418   intelligence that includes machine learning and deep learning in the hierarchy for image data
419   representation in cell analysis approaches. In addition, this review has listed the research gap for
420   future guidelines in Table 2.

Challenges in cell analysis approaches

Advanced technology exists to fulfil the current requirements with no intention of replacing the medical expert. Instead, the technology assists medical experts in making disease screening and diagnoses toward improving patient management. In general, most cell analyses still rely on manual methods performed by experts. However, conventional manual handling involves more handiwork with all the laboratory procedures that need to be well-organised and scrutinised for the lifetime of cell culture. Besides, the manual analysis performance could lead to error-prone, and it is very time-consuming. The researchers have tried to conduct several experimental works and research in developing an analysis system or application for cell and colony detection, classification, and counting. Cell analysis has monumental purposes in assisting for accurate and fast results, which explains the rationale that the advanced technology is needed. Considering that the Coulter counter implementation can provide excellent accuracies and is less time-consuming and reliable, it has been used in countless laboratory applications by average medical technology (Brecher, Schneiderman & Williams, 1956). In 1969, the Coulter counter (Model F) was applied in a cell suspension experiment to count red blood cells in mice's spleen colonies (Worton, Mcculloch & Till, 1969). This principle also became an industry foundation (Graham, 2003). Presently, Coulter Principle has been practically referred to as incorporating numerous numbers of automated cell counters. One of them is the Beckman Coulter instrument.

On the other hand, stem cell analysis is used for regenerative medicine and transplant, especially HSPC. CFU is crucially used to test in vitro functional assay of the haematopoietic system for HSPC differentiation of blood cell types into red blood cells, white blood cells, and platelet (Laurenti & Göttgens, 2018; Boyer et al., 2019). A standardisation of CFU assay has been evaluated in a previous report due to the poor reproducibility of the assay (Pamphilon et al., 2013). The Biomedical Excellent for Safer Transfusion (BEST) collaborative cellular therapy team initiates a survey to improve the CFU assay's reproducibility. According to their surveys, most of the laboratories respond to CFU assays incubated for 14-16 days with a performance of validation studies and consistency of inter-laboratory procedures. A semi-automatic device for the standardised quantification validation method of CFUs HSC has been conducted to accurately characterise the stem cell (Velier et al., 2019). Their research focuses on validating standard methods using the most designated computer software with an instrument developed by STEMCELL Technologies with the trademark STEMvision™. The experimental work of the manual method was compared with STEMvision™ on quantification counting of CFU using 20 mobilised apheresis, 17 samples from bone marrow, and 13 samples from cord blood. The result highlights that STEMvision™ meets high standard criteria than the manual method by reducing variance coefficients of recurring, varying inter-operator, and high capability in characterising the CFU HSC products.

The CCD digital camera was implemented in microscopic image acquisition with a high-quality sensor used in a camcorder as it consists of millions of micro solar cells in a 2D array, each of which converted the light into electrons. CCD has been used widely in several

460   experimental works for image acquisition as it can generate a high-quality image without
461   misinterpreting in charge transportation over the chips. For example, a CCD camera has been
462   used in stem cell-derived extracellular vesicles for super-resolution microscopic image
463   acquisition for MSCs analysis (Nizamudeen et al., 2018). The automated counting of MSCs by
464   implementing a deep learning approach using microscopic images was acquired using a CCD
465   digital camera and an inverted optical microscope (Hund Wetzlar) (Hassanlou, Meshgini &
466   Alizadeh, 2019). In 2019, a digital image of bone marrow cells was acquired using a CCD
467   camera of 20 megapixels (MP) on a single microscope (Yu et al., 2019). This research
468   automatically identified and classified 11 classes from bone marrow cells using DNN, with the
469   best achievement performed by erythroid lineage cells with 93.5% precision and 97.1% recall.
470   Ramji et al. have applied the CCD sensors to correlate with one pixel colour in high-resolution
471   image requirements (Ramji et al., 2020). Unlike conventional sensors such as CMOS, the chips
472   are manufactured traditionally like the standard microprocessors. Besides, CMOS tends to
473   generate low image resolution vulnerable to image noise.
474   Research gaps can be highlighted for automated system development in the review of cell
475   analysis approaches from the 16th century until the current approaches. Hitherto, the invention of
476   microscopes in minuscule observation has inspired scientists and researchers to develop a
477   physical instrument system for cell analysis based on photoelectronic and cell sorter techniques.
478   The achievement of instruments involves uncountable repeated experimental works using
479   laboratory apparatus incorporating electric circuits and an electronic device such as an oscillator.
480   The implementation took much longer working hours than expected to be carried out of
481   uncountable repeated experimental works and requires a high understanding of the multi-
482   disciplinary work of cytological and engineering expertise. The efforts of previous scientists and
483   researchers have motivated current researchers to carry out such trial and errors experimental
484   works of simulation to develop a system without the need for laboratory experiment tools. All
485   these opportunities could be implemented using digital visual sources such as images and videos
486   using image processing approach. However, the implementation of DIP requirements is
487   laborious and time constraints which involves multiple algorithms to select any significant input
488   feature for the final decision system, such as cell morphology features. Most of the DIP and
489   machine learning systems for cell analysation have semi-automated features for the system
490   requires an update for additional features.
491   Therefore, researchers realised the rationale behind the need for a system that
492   automatically updates the additional features without manual input, as the system can learn all
493   possible features through deep learning. Nevertheless, the requirements of any digital camera
494   tools are deniable for developing the automated system using the DL approach. The proposed
495   automated system from the reviewed section in "Automated cell analysis using deep learning"
496   can be referred to as a high potential framework point of view for future automated cell analysis
497   systems regardless of the variety of microscopic images. In fact, despite the large-scale data
498   requirements, the deep learning approach can reduce or eliminate manual feature extraction
499   requirements and achieve a high-performance system in cell analysis.

Conclusions

This review studies have briefly discussed cell analysis which covers identification and counting evolution by time using traditional, conventional, and automated approaches. Various cell analysis has been proposed and performed by scientists and researchers to develop better cell analysis techniques for the automated system. All these initiatives were rationally introduced with the priority objective to assist the experts/laboratories in automatically identifying and counting the cell without needing handcrafted analysis. It is also to meet the current high demand for system automation applications. Advanced cell analysis has evolved much faster than traditional analysis with high performance as its high demand in technology. Therefore, this field has vast potential, particularly for industrial applications, despite a significant data requirement. A more automated system will be developed in the future, and cell analysis approaches will be innumerable.

References

Abdolrasol MGM, Suhail Hussain SM, Ustun TS, Sarker MR, Hannan MA, Mohamed R, Ali JA, Mekhilef S, Milad A. 2021. Artificial neural networks based optimization techniques: A review. *Electronics* 10:2689–2731. DOI: 10.3390/electronics10212689.

Avior Y, Sagi I, Benvenisty N. 2016. Pluripotent stem cells in disease modelling and drug discovery. *Nature Reviews Molecular Cell Biology* 17:170–182.

Ball CS. 1966. The early history of the compound microscope. *Bios* 37:51–60.

Becker AJ, Mcculloch EA, Till JE. 1963. Cytological demonstration of the clonal nature of spleen colonies derived from transplanted mouse marrow cells. *Nature* 197:452–454.

Beznik T, Smyth P, Lannoy G de, Lee JA. 2022. Deep learning to detect bacterial colonies for the production of vaccines. *Neurocomputing* 470:427–431. DOI: 10.1016/j.neucom.2021.04.130.

Bhagavatula R, Fickus M, Kelly W, Guo C, Ozolek JA, Castro CA, Kovacevic J. 2010. Automatic identification and delineation of germ layer components in H&E stained images of teratomas derived from human and nonhuman primate embryonic stem cells. *In 2010 IEEE International Symposium on Biomedical Imaging: From Nano to Macro*:1041–1044. DOI: 10.1109/ISBI.2010.5490168.AUTOMATIC.

Bonner WA, Hulett HR, Sweet RG, Herzenberg LA. 1972. Fluorescence activated cell sorting. *Review of Scientific Instruments* 43:404–409. DOI: 10.1063/1.1685647.

Boyer SW, Rajendiran S, Beaudin AE, Smith-Berdan S, Muthuswamy PK, Perez-Cunningham J, Martin EW, Cheung C, Tsang H, Landon M, Forsberg EC. 2019. Clonal and quantitative in vivo assessment of hematopoietic stem cell differentiation reveals strong erythroid potential of multipotent cells. *Stem Cell Reports* 12:801–815. DOI: 10.1016/j.stemcr.2019.02.007.

Brecher G, Schneiderman M, Williams GZ. 1956. Evaluation of electronic red blood cell counter. *American Journal of Clinical Pathology* 26:1439–1449. DOI: 10.1093/ajcp/26.12.1439.

Buggenthin F, Buettner F, Hoppe PS, Endele M, Kroiss M, Strasser M, Schwarzfischer M, Loeffler D, Kokkaliaris KD, Hilsenbeck O, Schroeder T, Theis FJ, Marr C. 2017. Prospective identification of hematopoietic lineage choice by deep learning. *Nature*

541   *Methods* 14:403–406. DOI: 10.1038/nmeth.4182.

542 Cano E, Mendoza-Avilés J, Areiza M, Guerra N, Mendoza-Valdés JL, Rovetto CA. 2021. Multi
543   skin lesions classification using fine-tuning and data-augmentation applying NasNet. *PeerJ*
544   *Computer Science* 7:1–20. DOI: 10.7717/PEERJ-CS.371.

545 Chang YH, Abe K, Yokota H, Sudo K, Nakamura Y, Tsai MD. 2017. Human induced
546   pluripotent stem cell region recognition in microscopy images using convolutional neural
547   networks. *Biomedical Engineering - Applications, Basis and Communications*:4058–4061.
548   DOI: 10.4015/S1016237219500091.

549 Chow PW, Abd Hamid Z, Mathialagan RD, Rajab NF, Shuib S, Sulong S. 2021. Clastogenicity
550   and aneugenicity of 1,4-benzoquinone in different lineages of mouse hematopoietic
551   stem/progenitor cells. *Toxics* 9:1–17. DOI: 10.3390/toxics9050107.

552 Coons AH, Creech HJ, Jones RN. 1941. Immunological properties of an antibody containing a
553   fluorescent group. In: *Proceedings of the society for experimental biology and medicine*.
554   200–202. DOI: 10.3181/00379727-47-13084P.

555 Coulombel L. 2004. Identification of hematopoietic stem/progenitor cells: Strength and
556   drawbacks of functional assays. *Oncogene* 23:7210–7222. DOI: 10.1038/sj.onc.1207941.

557 Coulter WH. 1953. Means for counting particles suspended in a fluid. :1–9.

558 Coulter WH. 1956. High speed automatic blood cell counter and size analyzer. In: *Proceedings*
559   *of the national electronics conference*. 1034–1044.

560 Cram LS, Arndt-Jovin D. 2005. Mack Jett Fulwyler, pioneer of flow cytometry and flow sorting
561   (1936-2001). *Cytometry. Part A : The Journal of the International Society for Analytical*
562   *Cytology* 67:53–60. DOI: 10.1002/cyto.a.20176.

563 Crosland-Taylor PJ. 1953. A device for counting small particles suspended in a fluid through a
564   tube. *Nature* 171:37–38.

565 Dewi R, Hamid ZA, Rajab NF, Shuib S, Razak SA. 2020. Genetic, epigenetic, and lineage-
566   directed mechanisms in benzene-induced malignancies and hematotoxicity targeting
567   hematopoietic stem cells niche. *Human and Experimental Toxicology* 39:577–595. DOI:
568   10.1177/0960327119895570.

569 Van Dilla MA, Truiullo TT, Mullaney PF, Coultex JR. 1969. Cell microfluorometry: A method
570   for rapid fluorescence measurement. *Science* 163:1213–1214. DOI: 10.1016/s0033-
571   3506(57)80041-9.

572 Ebihara Y, Tsuji K, Lyman SD, Sui X, Yoshida M, Muraoka K, Yamada K, Tanaka R, Nakahata
573   T. 1997. Synergistic action of Flt3 and gp130 signalings in human hematopoiesis. *Blood*
574   90:4363–4368. DOI: 10.1182/blood.v90.11.4363.4363_4363_4368.

575 Fakunle ES, Loring JF. 2012. Ethnically diverse pluripotent stem cells for drug development.
576   *Trends in Molecular Medicine* 18:709–716. DOI: 10.1016/j.molmed.2012.10.007.

577 Fay FS, Carrington W, Fogarty KE. 1989. Three-dimensional molecular distribution in single
578   cells analysed using the digital imaging microscope. *Journal of Microscopy* 153:133–149.
579   DOI: 10.1111/j.1365-2818.1989.tb00554.x.

580 Fulwyler MJ. 1968. Particle separator. :1–9.

581 Graham MD. 2003. The coulter principle: Foundation of an industry. *JALA: Journal of the*
582   *Association for Laboratory Automation* 8:72–81. DOI: 10.1016/S1535-5535(03)00023-6.

583 Gregory PB, Milton RC, Johnson ML, Taura T. 1968. Spleen shielding in survivors of the atomic
584   bomb. *Radiation Research* 33:204–215. DOI: 10.2307/3572472.

585 Guan BX, Bhanu B, Talbot P, Lin S, Weng N. 2014. Comparison of texture features for human
586   embryonic stem cells with bio-inspired multi-class support vector machine. In:

587   *International conference on image processing (ICIP)*. 4102–4106.

588   Gucker Jr FT, O'Konski CT, Pickard HB, Pitts Jr JN. 1947. A photoelectronic counter for
589   colloidal particles. *Journal of the American Chemical Society* 69:2422–2431.

590   Gucker FT, O'Konski C. 1949. Electronic methods of counting aerosol particles. *Chemical*
591   *Reviews* 44:373–388. DOI: 10.1063/1.3047348.

592   Guyton AC. 1946. Electronic counting and size determination of particles in aerosols. *Journal of*
593   *Industrial Hygiene and Toxicology* 28:133–141.

594   Haden RL. 1939. The Origin of the Microscope. *Annals of Medical History* 1:30–44.

595   Haden RL. 1942. Galileo and the compound microscope. *Bulletin of the History of Medicine*
596   12:242–247.

597   Hajdu SI. 2002. A note from history: The first use of the microscope in medicine. *Annals of*
598   *Clinical and Laboratory Science* 32:309–310.

599   Hamid ZA, Sellappah P, Bharatham H, Mathialagan RD, Kannan VD. 2020. Role of N-acetyl
600   cysteine on bone marrow-derived hematopoietic stem/progenitor cell cryopreservation:
601   Outcome on the oxidative stress-mediated cryodamage and repopulation Capacity into
602   hematopoietic lineages. *Journal of Applied Pharmaceutical Science* 10:22–31. DOI:
603   10.7324/JAPS.2020.10604.

604   Harris D. 1911. The date of the discovery of the capillaries. *Nature* 86:584.

605   Hassanlou L, Meshgini S, Alizadeh E. 2019. Evaluating adipocyte differentiation of bone
606   marrow-derived mesenchymal stem cells by a deep learning method for automatic lipid
607   droplet counting. *Computers in Biology and Medicine* 112:103365–103403. DOI:
608   10.1016/j.compbiomed.2019.103365.

609   Hengen H, Spoor SL, Pandit MC. 2002. Analysis of blood and bone marrow smears using digital
610   image processing techniques. *In Medical Imaging 2002: Image Processing* 4684:624–635.

611   Hooke R. 1665. *Micrographia*. Royal society of London.

612   Jacobson LO, Marks EK, Gaston EO, Robson M, Zirkle RE. 1949. The role of the spleen in
613   radiation injury. *The Journal of Laboratory and Clinical Medicine* 70:740–742.

614   Jacobson LO, Simmons EL, Marks EK, Eldredge JH. 1951. Recovery from radiation injury.
615   *Science* 113:510–511.

616   Johnson JM, Khoshgoftaar TM. 2019. Survey on deep learning with class imbalance. *Journal of*
617   *Big Data* 6:1–54. DOI: 10.1186/s40537-019-0192-5.

618   Kavitha MS, Kurita T, Park SY, Chien S Il, Bae JS, Ahn BC. 2017. Deep vector-based
619   convolutional neural network approach for automatic recognition of colonies of induced
620   pluripotent stem cells. *PLoS ONE* 12:1–18. DOI: 10.1371/journal.pone.0189974.

621   Klug A, De Rosier DJ. 1966. Optical filtering of electron micrographs: reconstruction of one-
622   sided images. *Nature* 212:29–32.

623   Kobayashi K. 2002. "Birth of a digital phototelegraph-the Bartlane system-." *Journal of the*
624   *Institute of Image Electronics Engineers of Japan* 31:244–249. DOI:
625   10.11371/IIEEJ.31.244.

626   Kolios G, Moodley Y. 2013. Introduction to stem cells and regenerative medicine. *Respiration*
627   85:3–10. DOI: 10.1159/000345615.

628   Kusumoto D, Lachmann M, Kunihiro T, Yuasa S, Kishino Y, Kimura M, Katsuki T, Itoh S, Seki
629   T, Fukuda K. 2018. Automated deep learning-based system to identify endothelial cells
630   derived from induced pluripotent stem cells. *Stem Cell Reports* 10:1687–1695. DOI:
631   10.1016/j.stemcr.2018.04.007.

632   Kusumoto D, Yuasa S, Fukuda K. 2022. Induced pluripotent stem cell-based drug screening by

633   use of artificial intelligence. *Pharmaceuticals* 15. DOI: 10.3390/ph15050562.

634   Lane N. 2015. The unseen world: reflections on Leeuwenhoek (1677) "concerning little
635   animals." *Philosophical Transactions of the Royal Society B: Biological Sciences* 370:1–10.
636   DOI: 10.1098/rstb.2014.0344.

637   Laurenti E, Göttgens B. 2018. From haematopoietic stem cells to complex differentiation
638   landscapes. *Nature* 553:418–426. DOI: 10.1038/nature25022.

639   Leeuwenhoek A van. 1677. *Observations, Communicated to the Publisher by Mr. Antony van*
640   *Leewenhoeck in a Dutch Letter of the 9th Oct. 1676. Here English'd: concerning Little*
641   *Animals by Him Observed in Rain-Well-Sea. and Snow Water; as Also in Water Wherein*
642   *Pepper Had Lain Infused*.

643   Li Y, Liu T, Ceylan Koydemir H, Wang H, O'riordan K, Bai B, Haga Y, Kobashi J, Tanaka H,
644   Tamaru T, Yamaguchi K, Ozcan A. 2022. Deep learning-enabled detection and
645   classification of bacterial colonies using a thin film transistor (TFT) image sensor. *arXiv*
646   *preprint arXiv:2205.03549.*:1–18.

647   Lin HT, Otsu M, Nakauchi H. 2013. Stem cell therapy: An exercise in patience and prudence.
648   *Philosophical Transactions of the Royal Society B: Biological Sciences* 368:4–6. DOI:
649   10.1098/rstb.2011.0334.

650   Łos MJ, Skubis A, Ghavami S. 2018. Stem cells. In: *In Stem Cells and Biomaterials for*
651   *Regenerative Medicine*. Elsevier Inc., 5–16. DOI: 10.1016/B978-0-12-812258-7.00002-2.

652   Lowry N, Mangoubi R, Desai M, Marzouk Y, Sammak P. 2012. Texton-based segmentation and
653   classification of human embryonic stem cell colonies using multi-stage Bayesian level sets.
654   In: *International symposium on biomedical imaging*. 194–197. DOI:
655   10.1109/ISBI.2012.6235517.

656   Loya K. 2014. *Stem Cells*. Elsevier Inc. DOI: 10.1016/B978-0-12-386882-4.00011-6.

657   Maleki M, Ghanbarvand F, Behvarz MR, Ejtemaei M, Ghadirkhomi E. 2014. Comparison of
658   mesenchymal stem cell markers in multiple human adult stem cells. *International Journal*
659   *of Stem Cells* 7:118–126. DOI: 10.15283/ijsc.2014.7.2.118.

660   Mathe' G. 1959. Transfusions et greffes de moelle osseuse homologus chez des humains irradies
661   a hautes dose accidentellement. *Rev. Fr. Etudes Clin. Biol.* 4:226–238.

662   McCulloch EA, Till JE. 1960. The radiation sensitivity of normal mouse bone marrow cells,
663   determined by quantitative marrow transplantation into irradiated mice. *Radiation Research*
664   13:115–125. DOI: 10.2307/3570877.

665   McCulloch EA, Till JE. 1962. The sensitivity of cells from normal mouse bone marrow to
666   gamma radiation in vitro and in vivo. *Radiation research* 16:822–832. DOI:
667   10.2307/3571281.

668   Miah MS, Hossain Lipu MS, Ansari S, Meraj ST, Hasan K, Masaoud A, Hussain A, Mahmud
669   MS, Bashar SS. 2022. Energy storage controllers and optimization schemes integration to
670   microgrid: An analytical assessment towards future perspectives. *IEEE Access* 10:52982–
671   53014. DOI: 10.1109/ACCESS.2022.3174123.

672   Mie G. 1908. Article of the optical characteristics of turbid tubes, especially colloidal metal
673   solution. *Annalen der Physik* 25:377–445. DOI: 10.1002/andp.19083300302.

674   Mitra-Kaushik S, Mehta-Damani A, Stewart JJ, Green C, Litwin V, Gonneau C. 2021. The
675   evolution of single-cell analysis and utility in drug development. *AAPS Journal* 23:1–5.
676   DOI: 10.1208/s12248-021-00633-6.

677   Moldavan A. 1934. Photo-electric technique for the counting of microscopical cells. *Science*
678   80:188–189.

679 Nizamudeen Z, Markus R, Lodge R, Parmenter C, Platt M, Chakrabarti L, Sottile V. 2018. Rapid
680   and accurate analysis of stem cell-derived extracellular vesicles with super resolution
681   microscopy and live imaging. *Biochimica et Biophysica Acta - Molecular Cell Research*
682   1865:1891–1900. DOI: 10.1016/j.bbamcr.2018.09.008.
683 Ogi H, Moriwaki S, Kokubo M, Hikida Y, Itoh K. 2019. Label-free classification of neurons and
684   glia in neural stem cell cultures using a hyperspectral imaging microscopy combined with
685   machine learning. *Scientific Reports* 9:1–12. DOI: 10.1038/s41598-018-37241-y.
686 Oğuz O, Muenzenmayer C, Wittenberg T, Üner A, Çetin AE, Atalay RÇ. 2015. Detection of
687   cancer stem cells in microscopic images by using region covariance and codifference
688   method. *In 2015 International Workshop on Computational Intelligence for Multimedia*
689   *Understanding (IWCIM)*:1–5.
690 Packard FR. 1928. Marcello malpighi. *Annals of Medical History* 10:209–210.
691 Paduano V, Tagliaferri D, Falco G, Ceccarelli M. 2013. Automated identification and location
692   analysis of marked stem cells colonies in optical microscopy images. *PLoS ONE* 8:1–11.
693   DOI: 10.1371/journal.pone.0080776.
694 Pamphilon D, Selogie E, Mckenna D, Cancelas-Peres JA, Szczepiorkowski ZM, Sacher R,
695   McMannis J, Eichler H, Garritsen H, Takanashi M, Van De Watering L, Stroncek D, Reems
696   JA. 2013. Current practices and prospects for standardization of the hematopoietic colony-
697   forming unit assay: A report by the cellular therapy team of the Biomedical Excellence for
698   Safer Transfusion (BEST) Collaborative. *Cytotherapy* 15:255–262. DOI:
699   10.1016/j.jcyt.2012.11.013.
700 Pattanaik PA, Mittal M, Khan MZ, Panda SN. 2020. Malaria detection using deep residual
701   networks with mobile microscopy. *Journal of King Saud University - Computer and*
702   *Information Sciences* 34:1700–1705. DOI: 10.1016/j.jksuci.2020.07.003.
703 Ponti G, Muscatello U. 2015. The long road to the use of microscope in clinical medicine in
704   vivo: From early pioneering proposals to the modern perspectives of optical biopsy. *Acta*
705   *Medico-Historica Adriatica* 13:385–392.
706 Ramakrishna RR, Hamid ZA, Zaki WMDW, Huddin AB, Mathialagan R. 2020. Stem cell
707   imaging through convolutional neural networks: current issues and future directions in
708   artificial intelligence technology. *PeerJ* 8. DOI: 10.7717/peerj.10346.
709 Ramalho-Santos M, Willenbring H. 2007. On the origin of the term "stem cell." *Cell Stem Cell*
710   1:35–38. DOI: 10.1016/j.stem.2007.05.013.
711 Ramji DR, Palagan CA, Nithya A, Appathurai A, Alex EJ. 2020. Soft computing based color
712   image demosaicing for medical Image processing. *Multimedia Tools and Applications*
713   79:10047–10063. DOI: 10.1007/s11042-019-08091-1.
714 Ronneberger O, Fischer P, Brox T. 2015. U-Net: Convolutional networks for biomedical image
715   segmentation. In: *International conference on medical image computing and computer-*
716   *assisted intervention. Springer, Cham*. 234–241. DOI: 10.1007/978-3-319-24574-4.
717 Russakovsky O, Deng J, Su H, Krause J, Satheesh S, Ma S, Huang Z, Karpathy A, Khosla A,
718   Bernstein M, Berg AC, Fei-Fei L. 2015. ImageNet Large Scale Visual Recognition
719   Challenge. *International Journal of Computer Vision* 115:211–252. DOI: 10.1007/s11263-
720   015-0816-y.
721 Saraf PG, Cockett ATK. 1984. Marcello malpighi-A tribute. *Urology* 23:619–623.
722 Seita J, Weissman IL. 2010. Hematopoietic stem cell: Self-renewal versus differentiation. *Wiley*
723   *Interdisciplinary Reviews: Systems Biology and Medicine* 2:640–653. DOI:
724   10.1002/wsbm.86.

725 Shibata M, Okamura K, Yura K, Umezawa A. 2020. High-precision multiclass cell classification
726   by supervised machine learning on lectin microarray data. *Regenerative Therapy* 15:195–
727   201. DOI: 10.1016/j.reth.2020.09.005.
728 Siminovitch L, Mcculloch EA, Till JE. 1963. The distribution of colony-forming cells ampng
729   spleen colonies. *Journal of Cellular and Comparative Physiology* 62:327–336.
730 Sreedevi B, Pachaiammal PM. 2018. Analysis of performance metrics with mesenchymal stem
731   cell classification and optimization algorithms. In: *International conference on
732   communication, computing and Internet of Things (IC3IoT)*. 6–11.
733 Takahashi K, Yamanaka S. 2006. Induction of pluripotent stem cells from mouse embryonic and
734   adult fibroblast cultures by defined factors. *Cell* 126:663–676. DOI:
735   10.1016/j.cell.2006.07.024.
736 Tanaka A, Yuasa S, Mearini G, Egashira T, Seki T, Kodaira M, Kusumoto D, Kuroda Y, Okata
737   S, Suzuki T, Inohara T, Arimura T, Makino S, Kimura K, Kimura A, Furukawa T, Carrier
738   L, Node K, Fukuda K. 2014. Endothelin-1 induces myofibrillar disarray and contractile
739   vector variability in hypertrophic cardiomyopathy-induced pluripotent stem cell-derived
740   cardiomyocytes. *Journal of the American Heart Association* 3:1–25. DOI:
741   10.1161/JAHA.114.001263.
742 Tatullo M, Gargiulo IC, Dipalma G, Ballini A, Inchingolo AM, Paduanelli G, Nguyen C đăng K,
743   Inchingolo AD, Makeeva I, Scacco S, Nuzzolese M, De Vito D, Inchingolo F. 2019. Stem
744   cells and regenerative medicine. *Translational Systems Medicine and Oral Disease*:387–
745   407. DOI: 10.1016/B978-0-12-813762-8.00017-7.
746 Tbakhi A, Amr SS. 2007. Ibn Al-Haytham : Father of modern optics. *Annals of Saudi Medicine*
747   27:464–467. DOI: 10.4103/0256-4947.51450.
748 Till JE, Mcculloch EA. 1961. A direct measurement of the radiation sensitivity of normal mouse
749   bone marrow cells. *Radiation research* 14:213–222.
750 Twersky V. 1964. Rayleigh scattering. *Applied Optics* 3:1150–1162. DOI: 10.1364/ao.3.001150.
751 Velier M, Chateau A-L, Malenfant C, Ouffai S, Calmels B, Chabannon C, Lemarie C. 2019.
752   Validation of a semi automatic device to standardize quantification of colony-forming unit
753   (CFU) on hematopoietic stem cell products. *Cytotherapy* 21:820–823. DOI:
754   10.1016/j.jcyt.2019.06.005.
755 Wang H, Ceylan Koydemir H, Qiu Y, Bai B, Zhang Y, Jin Y, Tok S, Yilmaz EC, Gumustekin E,
756   Rivenson Y, Ozcan A. 2020. Early detection and classification of live bacteria using time-
757   lapse coherent imaging and deep learning. *Light: Science and Applications* 9:118–134.
758   DOI: 10.1038/s41377-020-00358-9.
759 Weissman IL. 2000. Stem cells: Units of development, units of regeneration, and units in
760   evolution. *Cell* 100:157–168. DOI: 10.1016/S0092-8674(00)81692-X.
761 Worton RG, Mcculloch EA, Till JE. 1969. Physical separation of hematopoietic stem cells
762   differing in their capacity for self-renewal. *The Journal of Experimental Medicine* 130:91–
763   103.
764 Wu AM, Till JE, Siminovitch L, McCulloch EA. 1968. Cytological evidence for a relationship
765   between normal hematopoietic colony-forming cells and cells of the lymphoid system. *The
766   Journal of Experimental Medicine* 127:455–464.
767 Wyatt PJ. 1969. Identification of bacteria by differential light scattering. *Nature* 221:1257–1258.
768 Wyatt PJ, Schehrer KL, Phillips SD, Jackson C, Chang Y-J, Parker RG, Phillips DT, Bottiger JR.
769   1988. Aerosol particle analyzer. *Applied Optics* 27:217–221. DOI: 10.1364/ao.27.000217.
770 Xiang J, Shi M, Fiala MA, Gao F, Rettig MP, Uy GL, Schroeder MA, Weilbaecher KN,

771   Stockerl-Goldstein KE, Mollah S, DiPersio JF. 2022. Machine learning–based scoring
772   models to predict hematopoietic stem cell mobilization in allogeneic donors. *Blood*
773   *Advances* 6:1991–2000. DOI: 10.1182/bloodadvances.2021005149.
774   Yu T-C, Chou W-C, Yeh C-Y, Yang C-K, Huang S-C, Tien FM, Yao C-Y, Cheng C-L, Chuang
775   M-K, Tien H-F, Zhang Q-Y, Hsu W-H, Chou S-C. 2019. Automatic bone marrow cell
776   identification and classification by deep neural network. *Blood* 134:2084–2086. DOI:
777   10.1182/blood-2019-125322.
778   Yuasa S, Fukuda K. 2008. Cardiac regenerative medicine. *Circulation Journal* 72:49–50. DOI:
779   10.1253/circj.CJ-08-0378.
780   Zakrzewski W, Dobrzyński M, Szymonowicz M, Rybak Z. 2019. Stem cells: Past, present and
781   future. *Stem Cell Research & Therapy* 10:1–22. DOI: 10.1541/ieejfms.128.329.
782   Zamani NSM, Zaki WMDW, Huddin AB, Hussain A, Mutalib HA, Ali A. 2020. Automated
783   pterygium detection using deep neural network. *IEEE Access* 8:191659–191672. DOI:
784   10.1109/access.2020.3030787.
785   Zhang J, Zhang J, Ding J, Lin Q, Young GM, Jiang C. 2022. Rapid identification of live and
786   dead Salmonella by surface-enhanced Raman spectroscopy combined with convolutional
787   neural network. *Vibrational Spectroscopy* 118:103332–103339. DOI:
788   10.1016/j.vibspec.2021.103332.

Figure 1

Figure 1: A block diagram of review methodology for this study
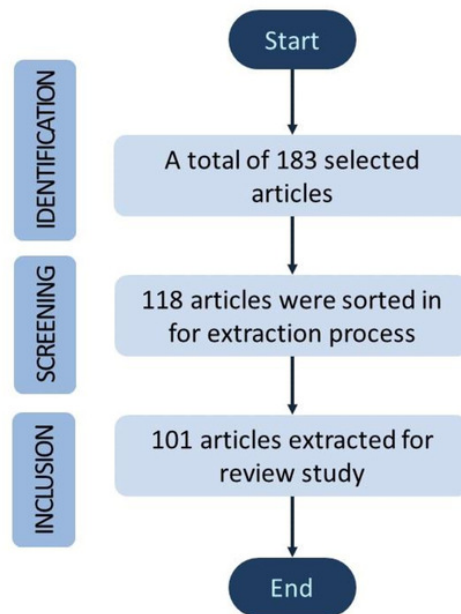
Figure 1: A block diagram of review methodology for this study

Figure 2

Figure 2: Evolution of the cell analysis approaches
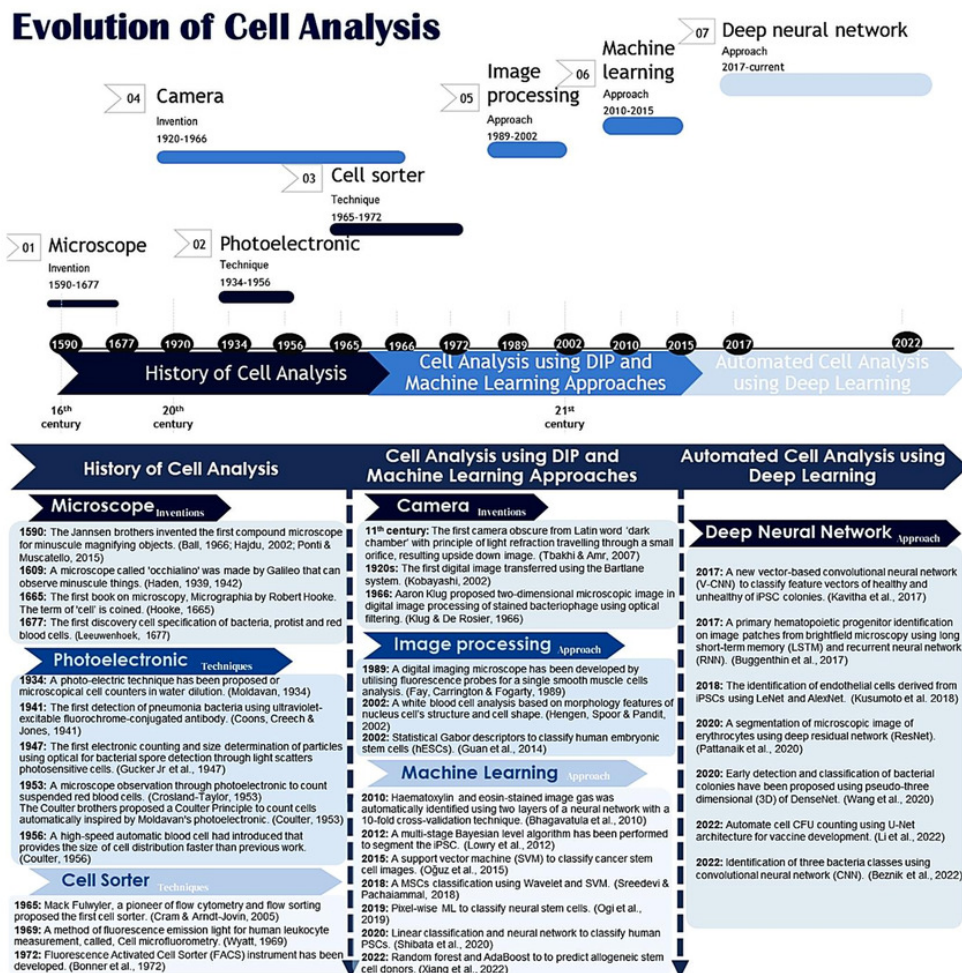
Figure 2: Evolution of the cell analysis approaches

Figure 3

Figure 3: Robert Hooke's invention and microscope discovery in Micrographia (Hooke, 1665) , a) a microscope and b) a thin slice of the cork (the origin 'cell' term were coined)

a)   b)
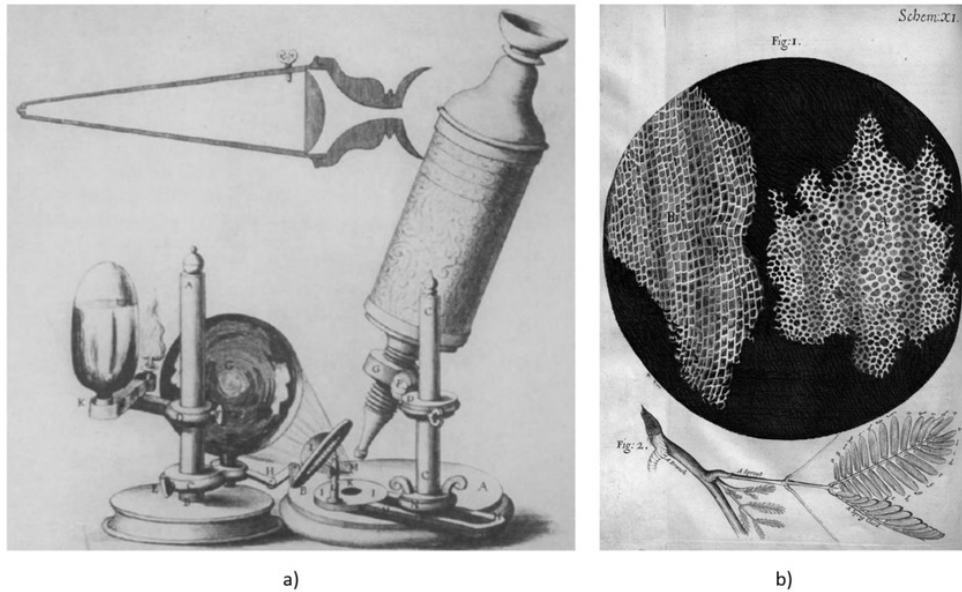
Figure 3: Robert Hooke's invention and microscope discovery in Micrographia (Hooke, 1665), a) a microscope and b) a thin slice of the cork (the origin 'cell' term were coined)

Figure 4

Figure 4: Illustration of schematic Coulter's photoelectronic counter (Coulter, 1956) .
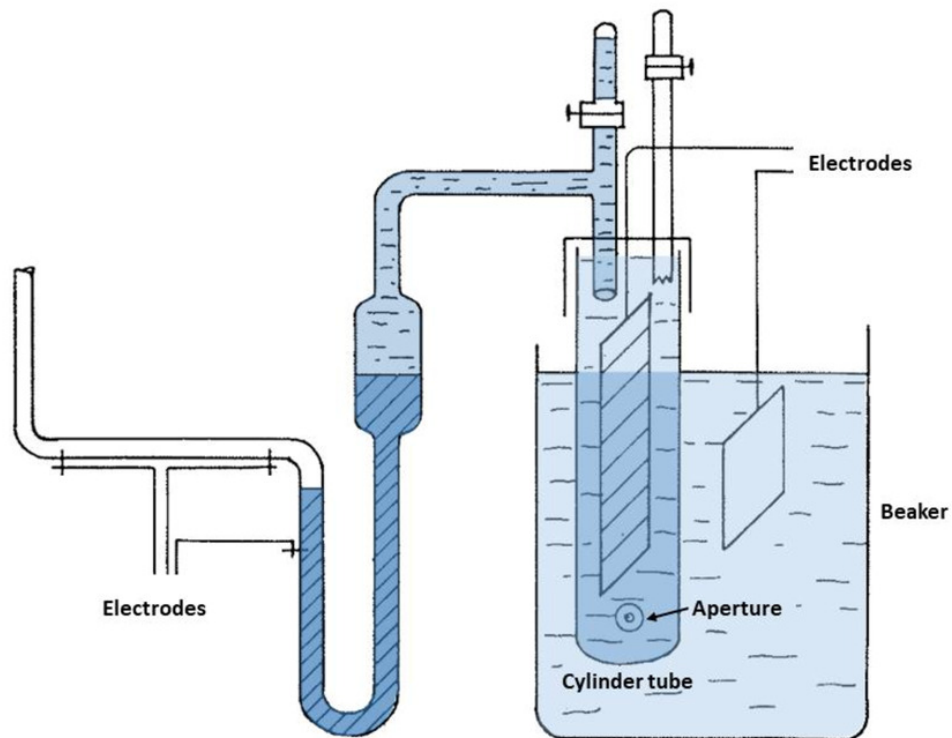
Figure 4: Illustration of schematic Coulter's photoelectronic counter (Coulter, 1956)

Figure 5

Figure 5: A cell sorter schematic (Bonner et al., 1972)
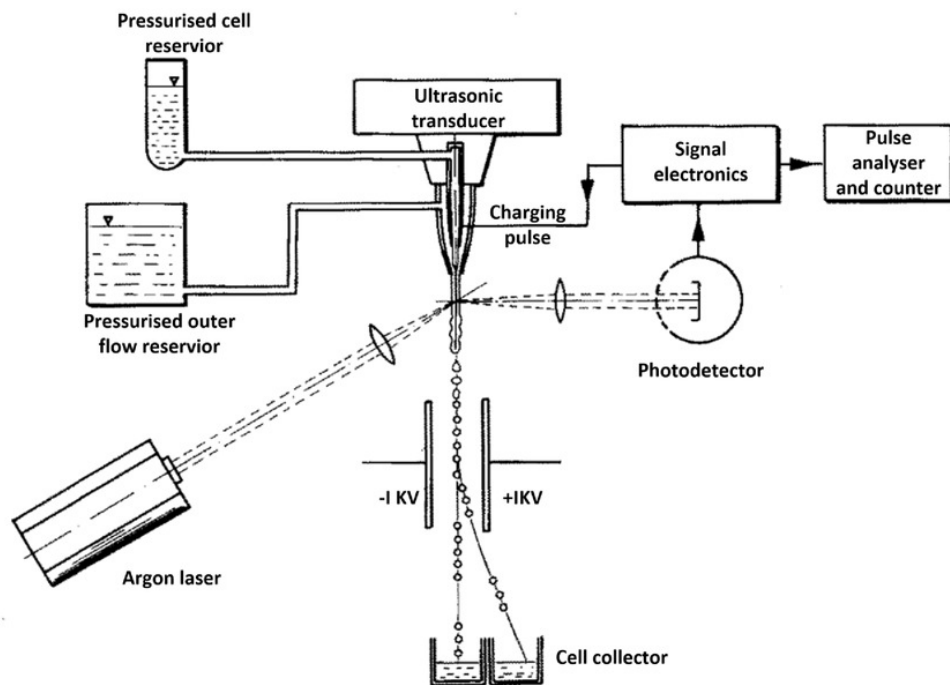
Figure 5: A cell sorter schematic (Bonner et al., 1972)

Figure 6

Figure 6: A hierarchy of computer vision and artificial intelligence
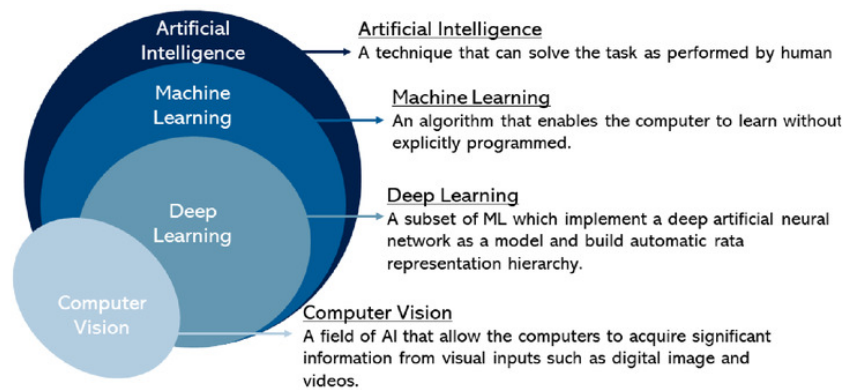
Figure 6: A hierarchy of computer vision and artificial intelligence

Table 1: Evolution of the cell analysis history

2 **Table 1**
3 Evolution of the cell analysis history

Ref.	Approach/ Methods	Cell/particle analysis				Advantages	Disadvantage
		Detection	Counting	Size measurement	Sorting		
(Moldavan, 1934)	Cells counting using photo-electric technique.		✔		✔	▪ Capable in microscopic cells counting.	▪ Faint visibility of microscopic cells. ▪ Need specific requirement tools for better result
(Coons et al., 1941)	The detection of pneumonia bacteria by an ultraviolet-excitable fluorochrome conjugated antibody.	✔				▪ Capable in clear pneumonia bacteria detection.	▪ Need understanding of fluorescence usage.
(Guyton, 1946)	Electronic counting and size determination of particles.	✔	✔	✔		▪ Capable in particle count and size measurement.	▪ Particle detection is not smaller than 2.5 µm. ▪ Rejected due to device sensitivity deficit.
(Gucker Jr et al., 1947)	Particles counter using photoelectronic.	✔	✔	✔		▪ Detect particles down to 0.6 µm.	▪ Need high understanding of complicated electric circuit.
(Gucker and O'Konski, 1949)		✔	✔	✔		▪ Improvement of particles visibility.	
(Crosland-Taylor, 1953)	A device for counting small particles suspended in a fluid through a tube.		✔	✔		▪ The first successful small particles counting in a fluid under microscopical observation with electronic counter alignment.	▪ High apparatus requirement.
(Coulter, 1953)	Means for counting particles suspended in a fluid.	✔	✔	✔		▪ The first automated cell counting based on Coulter Principle.	▪ Difficulties to obtain a perfect result. ▪ Requires calibration. ▪ High-cost and complex apparatus requirements.
(Coulter, 1956)	High-speed automatic blood cell counter and a cell size analyser.	✔	✔	✔		▪ Effective in cells detection and counting up to 6000 individual cells per second automatically. ▪ The minimum function of the oscilloscope and readily understood by average medical laboratories.	▪ Possibility cell loss count. ▪ The electronic circuit must be correctly connected.
(Fulwyler, 1968)	The first cell sorter.				✔	▪ Able to separate different types of cells.	▪ Requires understanding of complex circuit and apparatus design.

(Van Dilla et al., 1969)	Cell microfluorometry: a new method for the rapid measurement of biological cells stained with fluorescent dyes.	✔	✔			▪ Able to measure human leukocytes 104 to 105 cells per minute.	▪ Apparatus requirement to perform the cell measurement.
(Bonner et al., 1972)	The first Fluorescence Activated Cell Sorter (FACS) instrument.	✔	✔	✔	✔	▪ High result accuracies. ▪ The result can be obtained in an instant as the process was done.	▪ Slow stream flowing for FACS sorting. ▪ Expensive technology. ▪ Requires expertise to perform the analysis.

Table 2: Current approach of automated cell analysis using deep learning

1 **Table 1**
2 Current approach of automated cell analysis using deep learning

Ref.	Method	Cell analysis scope			Research Gap
		Identification	**Recognition/detection**	**Classification**	
Kavitha et al., 2017	▪ A new vector-based convolutional neural network (V-CNN) to classify a feature vector of healthy and unhealthy of iPSCs colonies. ▪ Undergo image segmentation and feature measurement to compute morphological and texture features. ▪ Comparison between the proposed V-CNN and SVM classifier by five-fold cross-validation.		✔		▪ V-CNN achieved high accuracy above 90% and the SVM classifier only 77%. ▪ V-CNN has outperformed the conventional classifier (SVM). ▪ High potential for reliable framework in automated recognition of iPSCs colonies. ▪ Quite challenging to compute the segmented colony region for the ensuing stem cell characteristics measurement.
Buggenthin et al., 2017	▪ Combination of CNN and LSTM of RNN for identification of hematopoietic progenitor. ▪ CNN adopted from LeNet structure. Three convolutional layers. Three max-pooling layers. Two fully connected layers. A softmax classifier for classification. ▪ For an RNN, the output of the extracted features is transferred to an LSTM with 20 hidden nodes.		✔		▪ Fast and robust for new data for training. ▪ Low level feature calculation requirement. ▪ However, the score of identification in not stated.
Chang et al., 2017	▪ Six classes microscopy images of iPSCs based on cell patterns. ▪ A region with no cells, separate cells, clustering cells, clustered cells, tightly clustered cells, and a region with iPSCs. ▪ CNN: Five convolutional layers and two fully connected layers		✔	✔	▪ Top-1 9.2% and Top-2 0.84% of error rates. ▪ The average time execution is 0.076 seconds approximately.
Kusumoto et al., 2018	▪ Adaption of two DNN architectures for identification of endothelial cells derived from iPSCs ▪ LeNet (two layers of convolutional network, max pooling and fully connected) ▪ AlexNet (five convolutional layers and three layers both max pooling and fully connected layer). ▪ A total of 800 images (600 images for training and 200 validation).	✔			▪ LeNet 70%: accuracy and F1 score ▪ AlexNet: 90% accuracy 75% F1 score

Reference	Description				Results
	▪ Network parameters are iteratively optimised.				
Pattanaik et al., 2020	▪ Modified deep residual network called multi-magnification ResNet (MM-ResNet) using erythrocyte microscopic image for malaria detection			✓	▪ Accuracy of 98.08 % slightly low compared to GoogleNet ▪ Outperformed GoogleNet in term of error rate.
Wang et al., 2020	▪ Utilised pseudo-3D DenseNet for bacterial colonies detection and classification. ▪ Use 4 time-consecutive frames in each time-lapse imaging. ▪ Image of bacterial colonies captured after incubation in 23.5 hours.		✓	✓	▪ Bacterial colonies >95% true detected within 12 hours. ▪ Precision (99.2-100%). ▪ Bacterial colonies classified at 80%.
Li et al., 2022	▪ Utilised a lens-free imaging modality using a TFT image sensor. ▪ A time-lapse of CFU images were automatically collected within 5 minutes on chromogenic agar plates. ▪ Detect and count colonies (E. coli and other coliforms) using two DNNs (DenseNet)		✓	✓	▪ CFU detection: 92.6% sensitivity 100% specificity ▪ CFU classification: 100% accuracy
Beznik et al., 2022	▪ Utilised U-Net architecture for multiple bacterial colonies segmentation and automated counting. Regular U-Net U-Net with a pre-trained encoder from ResNet-152		✓		▪ Detection of true positive of class Virulent (bvg+) and Avirulent (bvg-): Both scores were less than 74.5% ▪ Counting (Precision) Bgv+ (90.6%) Bgv- (91.9%)
Zhang et al., 2022	▪ Use surface-enhanced Raman spectroscopies (SERS) to detect three types of Salmonella bacterial colonies.	✓			▪ Stacking-CNN outperform all other models: Salmonella Typhimurium (98.31%), Salmonella Enteritidis (98.41%) Salmonella Paratyphoid (97.89%)